Simple shearing flow of dry soap foams with TCP structure

Douglas A. Reinelt

Department of Mathematics, Southern Methodist University, Dallas, Texas 75275-0156

Andrew M. Kraynik

Engineering Sciences Center, Sandia National Laboratories

Albuquerque, New Mexico 87185-0834

(May 3, 1999)

Abstract

The microrheology of dry soap foams subjected to large, quasistatic, simple shearing deformations is analyzed. Two different monodisperse foams with tetrahedrally close-packed (TCP) structure are examined: Weaire-Phelan (A15) and Friauf-Laves (C15). The elastic-plastic response is evaluated by calculating foam structures that minimize total surface area at each value of strain. The minimal surfaces are computed with the Surface Evolver program developed by Brakke. The foam geometry and macroscopic stress are piecewise continuous functions of strain. The stress scales as $T/V^{1/3}$ where T is surface tension and V is cell volume. Each discontinuity corresponds to large changes in foam geometry and topology that restore equilibrium to unstable configurations that violate Plateau's laws. The instabilities occur when the length of an edge on a polyhedral foam cell vanishes. The length can tend to zero smoothly or abruptly with strain. The abrupt case occurs when a small increase in strain changes the energy profile in the neighborhood of a foam structure from a local minimum to a saddle point, which can

DISCLAIMER

DISCLAIMER

Portions of this document may be illegible in electronic image products. Images are produced from the best available original document.

lead to symmetry-breaking bifurcations. In general, the new foam topology associated with each stable solution branch results from a cascade of local topology changes called T1 transitions. Each T1 cascade produces different cell neighbors, reduces surface energy, and provides an irreversible, film-level mechanism for plastic yield behavior. Stress-strain curves and average stresses are evaluated by examining foam orientations that admit strain-periodic behavior. For some orientations, the deformation cycle includes Kelvin cells instead of the original TCP structure; but the foam does not remain perfectly ordered. Bifurcations during subsequent T1 cascades lead to disorder and can even cause strain localization.

I. INTRODUCTION

The natural starting point for developing microrheological models of foam flow in three dimensions involves quasistatic deformation of a dry Kelvin foam (Reinelt & Kraynik 1993, 1996; Kraynik & Reinelt 1996). This parallels developments in two dimensions that can be traced to pioneering work on liquid honeycombs by Princen (1983). Film-level viscous flow that causes strain-rate dependence is absent under static conditions where minimizing surface energy is the dominant physical mechanism. The film-level geometry is simplest in the hypothetical dry limit because the foam structure is composed entirely of minimal surfaces that define the faces of polyhedral cells. Plateau borders, which form along cell edges in wet foams, are absent in dry foams where they degenerate to the intersection of three surfaces as the liquid volume fraction goes to zero. The dry foam based on the Kelvin cell (see Fig. 1) is the only known structure composed of identical polyhedra that is known to satisfy Plateau's laws in 3D (just like the hexagonal cell in 2D). The most elementary models that provide a baseline for further developments only include one polyhedron in the representative volume of foam, which is commonly referred to as the unit cell. Even under arbitrary homogeneous deformation the Kelvin foam only has seven unique faces when constrained by perfect order. Unless otherwise stated, a Kelvin foam will refer to the elementary model based on one polyhedron in the unit cell.

This analysis extends previous investigations of foam flow in 3D by considering more complicated cell arrangements that include several polyhedra in the unit cell. Multiple polyhedra lift many of the inherent constraints of perfect order. We consider two structures composed of several different equal-volume cells: Weaire-Phelan and Friauf-Laves, which are also known as A15 and C15, respectively. Both belong to a class of two dozen or so structures known as tetrahedrally close-packed (TCP) to crystallographers and Frank-Kasper to metallurgists and material scientists (Rivier 1994). The rheological response includes several features expected of all dry foams. The stress-strain curves are piecewise continuous, which corresponds to elastic-plastic behavior. Each branch of the curve represents large-

deformation elastic response of a foam with fixed topology, *i.e.*, the behavior is reversible and cell neighbors do not change. Each branch terminates when the foam structure violates topological constraints on edge and face connectivity that are contained in Plateau's laws. Stability is restored by a cascade of local topology changes that result in a stable foam structure with different cell neighbors. The jumps in stress and structure are not reversible.

In a perfectly ordered foam, each branch of the stress-strain curve involves Kelvin cells and the types of topology changes are severely restricted. In contrast, topology changes in TCP foams produce a broad range of cell types. The following analysis focuses on these and other microrheological mechanisms and phenomena that arise in simple multi-cell systems.

II. EVOLUTION OF FOAM STRUCTURE WITH SHEAR

The structure of a dry foam under static conditions satisfies Plateau's laws and consists of a continuous network of films with uniform surface tension T and constant mean curvature. In general, the mean curvature varies between films because the cells have different internal pressure. The films are stabilized against rupture by the presence of surfactants, *e.g.*, the soap in a soap froth. The volume fraction of continuous liquid phase is zero in the dry limit. Plateau-border channels that form along cell edges in wet foams are absent. The shape of each film satisfies the Young-Laplace equation

$$\Delta p = 2\,T\,(\nabla \cdot \mathbf{n}) \tag{1}$$

where Δp is the pressure difference between adjacent bubbles, $\mathbf{n}$ is a local unit vector normal to the dividing film, and the term in parentheses is the sum of the principal curvatures. The factor of two accounts for both film interfaces. To balance forces and minimize energy, three films intersect along cell edges at equal dihedral angles of 120° and four edges meet at each vertex at equal tetrahedral angles of $\cos^{-1}(-1/3) = 109.47°$. These equilibrium conditions are called Plateau's laws; they were deduced from experimental observation (Plateau 1873) and eventually shown to be a mathematical consequence of minimizing surface area (Taylor 1976).

The assumption that the volume of individual cells remains constant during simple shearing flow requires justification that is unnecessary for a Kelvin foam. In general, the pressure of each cell depends on the size, shape, and topology of it and its neighbors. The resulting pressure differences Δp drive gas diffusion between cells, which causes well-known coarsening phenomena. We neglect this diffusion, which can be slow compared to the foam deformation rate. Independent of gas diffusion, the cell pressures change with their geometry as the foam deforms. This occurs even when the total volume of foam is constant under simple shear. We neglect variations in cell volume due to these deformation-induced pressure fluctuations. This "incompressibility" assumption is valid for foams with large bubbles where the surface energy density is small compared to the average cell pressure.

The representative volume of a spatially periodic system is defined by a parallelepiped formed by three lattice vectors, $\mathbf{L}_i$. The undeformed Weaire-Phelan (WP) foam shown in Fig. 1 has the smallest known surface area of any structure with equal-volume cells (Weaire & Phelan 1994). It contains eight distinct bubbles with two different topologies. Six tetrakaidecahedra with two hexagonal and twelve pentagonal faces are arranged in mutually perpendicular columns that are aligned with a simple cubic lattice. Single pentagonal dodecahedra fit in between these columns. For orientation 1 of the WP foam, we align the cubic lattice with the coordinate axes

$$\begin{aligned} \mathbf{L}_1 &= 2V^{1/3}\ (1,0,0) \\ \mathbf{L}_2 &= 2V^{1/3}\ (0,1,0) \\ \mathbf{L}_3 &= 2V^{1/3}\ (0,0,1)\ . \end{aligned} \tag{2}$$

Here, the x-axis points to the right, the y-axis points up, and the z-axis points out of the page.

The undeformed Friauf-Laves (FL) foam also shown in Fig. 1 contains six distinct bubbles with two different topologies. There are four pentagonal dodecahedra and two 16-hedra with four hexagonal and twelve pentagonal faces. The Friauf-Laves foam has face-centered cubic (FCC) structure. For orientation 1, we choose

$$\mathbf{L}_1 = \sqrt{2}(3V)^{1/3}\ (1,0,0)$$
$$\mathbf{L}_2 = \sqrt{2}(3V)^{1/3}\ (1/2,\sqrt{2/3},-\sqrt{3}/6)$$
$$\mathbf{L}_3 = \sqrt{2}(3V)^{1/3}\ (1/2,0,-\sqrt{3}/2)\ . \tag{3}$$

These vectors coincide with the edges of a regular tetrahedron.

We consider homogeneous simple shear in the xy-plane. This is accomplished by applying a deformation gradient $\mathbf{F}$ to the lattice vectors, where

$$\mathbf{F} = \begin{bmatrix} 1 & \gamma & 0 \\ 0 & 1 & 0 \\ 0 & 0 & 1 \end{bmatrix} \tag{4}$$

and γ is the shear strain. We can think of γ as dimensionless time, when the shear rate $\dot{\gamma}$ is constant. The capillary number Ca expresses the relative importance of viscous to surface tension forces and is defined as

$$Ca = \frac{\mu\dot{\gamma}V^{1/3}}{T} \tag{5}$$

where μ is the liquid viscosity. In the quasistatic regime under consideration, Ca is zero.

The foam is deformed by increasing the shear strain in small increments $\Delta\gamma$. At each value of γ, the structure with minimal surface area is computed. The shear strain is increased until a solution that satisfies Plateau's laws cannot be found. This point of instability, an elastic limit, is always associated with a shrinking edge on a shrinking face; but, the edge length does not necessarily go smoothly to zero with strain. Stability is restored by topological transitions (T1s) that result in a foam with different geometry and lower surface area.

Foam structures with minimal area were calculated with the Surface Evolver program developed by Brakke (1992). The Surface Evolver converges to a minimal surface by simulating the process of evolution by mean curvature. Each n-sided face is subdivided into n triangular facets with a common vertex in the interior of the face. The shape of each facet is

approximated by a quadratic function. To verify that this level of refinement was adequate for our purposes, further refinements were also performed.

To simplify calculations, foam orientations are chosen so that the lattice is strain-periodic. The orientations represented by (2) and (3) give the smallest strain period for each lattice under simple shear. Other cases involve lattice rotation before deformation. The foam orientations that are analyzed here do exhibit strain-periodic behavior; however, the period of the lattice and the foam can be different. In general, strain-periodic lattice response does not guarantee strain-periodic evolution of foam structure. The particular orientations that we examine not only minimize the range of strain that needs to considered, but they also maximize the distance between identical "image" cells on the lattice. This reduces some artifacts of spatially periodic models, such as large distortions that occur when images are very close.

III. MACROSCOPIC STRESS

The effective, macroscopic stress tensor σ for the foam is calculated by averaging the local, position-dependent stress over the unit cell. The stress for a dry foam with equal-volume cells under static conditions is obtained from

$$\sigma = -\frac{1}{N}\sum_{k=1}^{N} p_k \, \mathrm{I} + \frac{T}{NV}\sum_{i=1}^{2F}\iint_{S_i}(\mathrm{I}-\mathbf{nn})\, da \tag{6}$$

where p_k is the pressure inside the k^{th} bubble, V is the volume of each of the N bubbles, I is the identity tensor, and da is the differential area element of the i^{th} film. There are twice as many interfaces as films F since each film has two sides. The shear stress σ_{xy} can be evaluated from the local stress using (6) or it can be evaluated from the surface energy using

$$\sigma_{xy} = \frac{T}{NV}\frac{dS}{d\gamma} = \frac{T}{NV}\frac{d}{d\gamma}\sum_{i=1}^{2F} S_i \tag{7}$$

where S is the total surface area of N bubbles and S_i refers to the i^{th} interface. Our calculations using the two methods give consistent results. In all calculations, we set the

cell volume V equal to one, which is equivalent to scaling length by $V^{1/3}$. Stress and energy density are scaled by $T/V^{1/3}$.

For spatially periodic foams, viscometric functions are evaluated by averaging the instantaneous stress over time. When the foam structure and stress are strain-periodic,

$$\overline{\sigma} = \frac{1}{\gamma_F} \int_{\gamma}^{\gamma+\gamma_F} \sigma \, d\gamma \tag{8}$$

where σ is the instantaneous stress given in (6), $\overline{\sigma}$ is the time-averaged stress, and γ_F is the strain period of the foam. The time-averaged shear stress can also be evaluated from σ_{xy} in (7).

IV. TOPOLOGICAL TRANSITIONS

A. Basic T1 transitions

As a dry foam deforms, the length of edges and the area of faces can increase or decrease. When a length goes to zero, more than four edges meet at the new, combined vertex. This violates Plateau's laws and provokes topological transitions, which have been called 'rearrangements in polyhedric foam' by Schwarz (1964). Weaire & Fortes (1994) have discussed T1 transitions in 2D and 3D.

There are two ways for an edge to vanish and they both occur frequently. First, the length can go smoothly to zero with strain. To calculate the critical strain, we compute the length of the shortest edge at three values of strain near the critical strain and extrapolate. The other way for an edge to vanish starts out similar to the first with length decreasing smoothly. Then, with a very small increase in strain, the edge suddenly vanishes. This abrupt onset of transition will be examined in the next section.

The loss of edges triggers three basic T1 transitions that depend on the foam geometry. These transitions are completely specified as long as it is clear which edge vanishes first. Our discussion of topological transitions will focus on the foam geometry in the vicinity of an edge, as shown in Fig. 2. We refer to the three bubbles that form a particular edge as

"edge" bubbles. These bubbles are separated by three faces that share that edge. Each vertex of the edge involves another bubble. We refer to these as "end" bubbles. Six faces separate end bubbles from edge bubbles.

The first basic T1 transition involves end bubbles moving toward each other. When the intervening edge vanishes, the end bubbles touch at a combined vertex where six edges now meet (see Fig. 2). The unstable vertex splits into three vertices that define a new triangular face; this face is shared by new neighbors–the original end bubbles. The three faces that separated edge bubbles have lost an edge and the six faces that separated end bubbles from edge bubbles have gained an edge. The outcome of this edge-to-triangle (ET) transition is well defined.

Triangular faces are rare in stable foams that are reasonably monodisperse. Usually an edge-to-triangle transition is followed by at least one and possibly many more transitions before a stable foam stucture is achieved. We refer to this sequence as a cascade of transitions.

The second basic T1 transition, triangle-to-edge (TE), is the reverse of an edge-to-triangle transition (see Fig. 2). A triangular face that separates two bubbles shrinks toward a point. When the face vanishes, its vertices converge to form an unstable six-way vertex, which splits to form two new four-way vertices and a new edge.

The third basic T1 transition, quadrilateral-to-quadrilateral (QQ), occurs when opposite edges of a quadrilateral face vanish at the same time. The face degenerates to form an edge as shown in Fig. 3. Both vertices of the new edge have a valence of five and the edge connects four faces that separate four bubbles. Two of these bubbles were neighbors that shared the shrinking face; the other two bubbles were not neighbors before the face collapsed. Stability is restored when the original neighbors separate by drawing a new quadrilateral face from their common edge. The new neighbors share the new face. Viewed in cross section, this topological transition resembles the fundamental T1 in two dimensions (see Fig. 3).

In a Kelvin foam, every edge borders one quadrilateral face and two hexagonal faces. Furthermore, opposite edges of every face always have the same length. Consequently, the

QQ transition is the most common in a Kelvin foam and has been referred to as the standard transition in that case (Reinelt & Kraynik 1996).

In foams with less symmetry, opposite edges of a quadrilateral often shrink but do not vanish simultaneously. In this situation, an ET transition is followed immediately by a TE transition; this sequence produces the same result as a QQ transition. The ET transition eliminates one edge from the quadrilateral face leaving a triangular face that continues to shrink. The vanishing edge also produces a second triangular face. The TE transition eliminates the shrinking triangle and adds an edge to the other triangle, which creates the new quadrilateral face.

Sometimes all four edges of a quadrilateral shrink simultaneously. In this case the quadrilateral tends toward a point instead of a line segment. Here, it can be difficult to determine with certainty which of the four edges vanishes first. For certain deformations of a Kelvin foam, all four edges on a quadrilateral are identical so the face shrinks precisely toward a point. We have called this situation a point transition. There are two possible outcomes that are equivalent to choosing which set of opposite edges on the quadrilateral vanished first. In a Kelvin foam, the resulting structures are mirror images. In TCP foams, a point transition can result in two, very different structures. If the two smallest edges are opposite edges, we assume that they disappear first. If they are adjacent, we examine both alternatives.

B. Symmetry-breaking bifurcations

TCP foams have less symmetry than Kelvin foams but they still have a lot. The pentagonal dodecahedra in Weaire-Phelan and Friauf-Laves foams are centrosymmetric, *i.e.*, points opposite the center correspond. This symmetry is preserved under homogeneous deformation as long as the topology does not change. The other polyhedra in these foams are not centrosymmetric. Nonetheless, for each edge and pentagonal face on one of these cells there is a corresponding feature with the same dimensions on a neighboring cell of the same type.

Consider two corresponding edges of equal length that shrink with strain as the minimal foam structure evolves. Usually, a small increase in strain slightly shifts the local minimum and the new structure is very close to the previous structure. If this continues, the edges will vanish smoothly with strain. Alternatively, a small increase in strain could change the neighborhood of the solution from a local minimum to a saddle point. If this occurs, the new stable structure will not be close to the previous one. In fact, every time that this occurred in our TCP simulations, at least one edge disappeared leading to a T1 transition and a new foam structure. This is the mechanism by which an edge vanishes abruptly.

In some cases, the saddle.point simply accelerates a transition that would occur if edges vanished smoothly. In other cases, there is a bifurcation that breaks symmetry. Figure 4 illustrates how a bifurcation occurs. Each curve represents a particular value of strain with strain increasing in increments of 0.01 from the bottom to the top of the figure. The energy is plotted against the length of one of two small edges. In other words, at each point along the curve, the length of one edge is specified and the foam structure with minimal energy is determined subject to this constraint. The other edge is free to have different length; the two small edge lengths are determined by a horizontal line that intersects the energy curve. We note that the distance between curves has been reduced substantially to fit them on the same plot. Variations in energy along a single curve are $O(10^{-4})$ while variations in energy between curves are $O(10^{-2})$.

The minimum energy on the lowest curve corresponds to an equilibrium foam structure (no constraints). Here, the two small edges have equal length. A small increase in strain shifts the local minimum and the new foam structure is close to the original one but the lengths have decreased. Eventually, the solution with equal edge lengths is no longer a local minimum; one edge will now vanish as the other grows. We note that the curves shown in Fig. 4 only represent one class of foam structures and that the local maxima are actually saddle points when all possibilities are considered. Either one of the two small edges can vanish depending on the direction that one leaves the saddle point. This leads to bifurcation.

In this particular example, it is not possible for both small edges to vanish simultaneously.

If we constrain both small edges to have equal length, then the energy is larger than the saddle point. This is not always the case. Sometimes, the appearance of a saddle point, where there used to be a local minimum, does lead to both small edges vanishing simultaneously. In this case, a symmetry breaking bifurcation does not occur.

Note that just after the local minimum changes to a saddle point, the steepest descent direction away from the saddle point is not very steep. Consequently, it takes many iterations of the Surface Evolver to confirm that the difference between the small lengths is substantial and increasing monotonically.

It is more difficult to diagnose bifurcations when they occur in the middle of a T1 cascade. The first transition can result in an unstable structure with many vanishing edges. When it is not clear whether two equivalent edges vanish simultaneously and preserve symmetry or only one vanishes, we examine both possibilities. When only one edge disappears first, we examine the other edge to see if it continues to shrink or begins to grow in size. If the other edge grows after the first edge vanishes, this is a good sign that there is a symmetry breaking bifurcation. If it continues to shrink and vanishes, one gets the same foam structure as when both edges disappear simultaneously.

A second test is to follow the two possibilities through to the end of a cascade. If the energy of the symmetric structure is much higher than the less symmetric structure and the shape of the bubbles and films are highly distorted then we conclude that the less symmetric structure is preferred. If the energies of two paths are comparable, we assume that both paths are possible and follow each separately.

Some orientations of TCP foams (orientation 1 of the Weaire-Phelan foam and orientation 2 of the Friauf-Laves foam) possess mirror symmetry across the shear plane. This symmetry is preserved under simple shear in the cases that we examined.

V. RESULTS FOR WEAIRE-PHELAN FOAM

Two strain-periodic orientations are examined for each foam. In all cases, simple shear is applied according to the deformation gradient in (4). Orientation 1 of the Weaire-Phelan foam (WP1) corresponds to the lattice vectors in (2). The columns of 14-hedra are aligned with the coordinate axes, *e.g.*, the x-column bubbles are aligned with the x-axis. Six of the eight bubble centers lie in two, horizontal layers (xz-planes); *i.e.* the z-column bubbles (Z_1 and Z_2) and one dodecahedron (D_1) lie in the 'lower' layer and the x-column bubbles (X_1 and X_2) and the other dodecahedron (D_2) lie in the 'upper' layer. One y-column bubble (Y_1 or Y_2) is centered half way in between the alternating layers.

Under simple shear the lattice for WP1 has a strain period of unity. Figure 5 shows the deformed foam at $\gamma = 0.65$ just before the first topological transition (see Fig. 1 for the initial structure). The first two T1 cascades are initiated by single or multiple edges vanishing smoothly. Both cascades can be divided into two steps (see Table I). To simplify the table, we have listed quadrilateral-to-quadrilateral (QQ) transitions whenever possible, even if the opposite edges are not exactly the same length. As discussed above, these transitions can be split into an edge-to-triangle (ET) transition followed by a triangle-to-edge (TE) transition.

The layered structure persists up until the third and final cascade, even though the topology of individual polyhedra changes. The final cascade begins with a symmetry-breaking bifurcation that causes y-column bubbles to 'combine' with the layer immediately above or below. This cascade results in a foam with Weaire-Phelan topology (see Table I).

We did not anticipate that the strain period of the lattice γ_L and the strain period of foam γ_F would coincide. If the bubble centers moved with the mean flow, *i.e.*, their motion was affine, it would take a strain of four for every bubble, *e.g.* X_1, to occupy the original position of an image. This is a consequence of bubble centers being located on four, different, equally spaced y-levels. The foam has $\gamma_F = 1$ because the bubbles do not move affinely, but change relative positions and even change type over a cycle. The bifurcation determines which bubbles are 'shuffled' at the end of a cycle (see Table I); there are two possibilities

depending on whether the y-column bubbles move up or down.

Figures 6 and 7 contain the shear stress and normal stress differences for WP1. The latter are defined according to the standard convention for viscometric functions: $N_1 = \sigma_{xx} - \sigma_{yy}$ and $N_2 = \sigma_{yy} - \sigma_{zz}$. Note that the foam never returns to an *undeformed* Weaire-Phelan structure with isotropic stress. This is because the last transition occurs at a shear strain greater than $\gamma = 1$.

The next shortest strain period for a cubic lattice is $\gamma_L = \sqrt{2}$. This orientation (WP2) is equivalent to flow along a diagonal of a face of a cube; it is obtained by rotating WP1 45° about the y-axis. Rotating in different directions results in structures that are mirror images but these have the same shear stress σ_{xy} and normal stress differences. The sign of the other shear stress components does depend on rotation direction. The first T1 cascade begins with two edges vanishing smoothly. This is followed by two quadrilateral faces shrinking to a point. As discussed in the previous section, each point transition has two possible outcomes. For Kelvin foams, the resulting structures are mirror images with respect to the xy-plane and have the same shear stress σ_{xy}. Here, there are four possible combinations for the double-point transition of WP2. Two of these break symmetry and differ depending on whether y-column bubbles move up or down. We will refer to them as WP2a since they have the same σ_{xy} (see Fig. 8). The second T1 cascade begins when two edges vanish smoothly. The third cascade is provoked by an abrupt saddle-point transition. The fourth cascade begins with a symmetry-breaking bifurcation where one of two quadrilaterals abruptly shrinks to a point. This bifurcation also determines whether y-column bubbles move up or down. The final T1 cascade restores Weaire-Phelan structure. Like WP1, the stress is not isotropic, the strain period of the lattice and foam are the same, and bubbles are shuffled. Two bifurcations per cycle lead to four different shufflings in WP2a.

A. Case WP2b: Weaire-Phelan to Kelvin

The other possibilities for the double-point transition do not break symmetry about the xy-plane; we refer to them as WP2b. The response eventually becomes periodic, as indicated by the stress-strain curve in Fig. 9. This case exhibits several phenomena that have not been observed previously. The cycles do not involve any Weaire-Phelan structure, even though it was the initial topology of the foam. At some point the foam becomes perfectly ordered: a T1 cascade at $\gamma = 2.69$ produces eight identical polyhedra, which must be Kelvin cells (see Fig. 9).

Elementary models based on the Kelvin cell only include one polyhedron in the unit cell. This eliminates the possibility of any other stable structure but Kelvin–the foam cannot escape perfect order. The presence of multiple polyhedra in the unit cell provides additional degrees of freedom. This permits bifurcations that break symmetry and lead to more complex structure. Figure 9 also shows the outcome of the next cascade at $\gamma = 3.21$ in which Kelvin cells are transformed into different polyhedra. This bifurcation is caused by a local energy minimum changing to a saddle point.

Four more T1 cascades restore perfect order near $\gamma = 3.80$. The resulting Kelvin cells become highly distorted and the stress grows very large, as shown in Fig. 9. This occurs because hexagonal faces separate cells that are being pulled apart. This situation is similar to the triple transition discussed by Reinelt & Kraynik (1996).

The foam now consists of Kelvin cells equally distributed between horizontal layers. The next cascade near $\gamma = 5.30$ involves identical QQ transitions on each cell triggered by edges vanishing smoothly. Since there are no bifurcations, the response could be captured by a single-cell model, but the following cascade at $\gamma = 5.54$ is very different. A bifurcation leads to QQ transitions in alternate layers of cells. The resulting intermediate structure is neither stable nor perfectly ordered. Additional T1 transitions at the same level restore perfect order. Even though the initial and final structures consist of Kelvin cells, this response could not be captured by a single-cell model because the foam undergoes strain localization.

All cell-neighbor switching occurs at alternate levels between layers; the cell topology at the other levels is undisturbed. Consequently, foam layers that are two cells thick glide past one another. This completes the first cycle. Unlike WP1 and WP2a, the foam period is twice the lattice period, $\gamma_F = 2\gamma_L = 2\sqrt{2}$, and the cycle does not involve Weaire-Phelan structure.

VI. RESULTS FOR FRIAUF-LAVES FOAM

Orientation 1 of the Friauf-Laves foam (FL1) corresponds to the FCC lattice in (3). This lattice has equilateral triangles covering the xz-plane. The triangle sides specified by $\mathbf{L}_1$ are aligned with the flow along the x-axis. The lattice response is strain periodic with $\gamma_L = \sqrt{3/2}$, the smallest possible value for an FCC lattice. This orientation is similar to case WP2b: the cycles do not involve Friauf-Laves structure, but they do involve Kelvin cells and the foam does not remain perfectly ordered.

The third T1 cascade for FL1 includes bifurcations caused by point transitions that result in two different periodic solutions (see Figs. 10 and 11). One case FL1a follows two slightly different paths to the same periodic solution with $\gamma_F = 3\gamma_L/2$ as shown in Fig. 10. In the other case FL1b, the period of the foam and the lattice are equal (see Fig. 11).

Rotation of FL1 about the y-axis by $\pm 30°$ generates two different structures with the same lattice, which have $\gamma_F = \gamma_L = 3/\sqrt{2}$. FL2a obtained by rotating $+30°$ and Fl2b obtained by rotating $-30°$ are not mirror images of each other. The stress-strain behavior of FL2a and FL2b are related by a phase shift equal to one third of the lattice period, as shown in Fig. 12. The first of four T1 cascades for FL2a begins at $\gamma = 0.93$ when four edges vanish smoothly. This cascade produces a deformed foam with Friauf-Laves topology, which becomes FL2b if the strain is reduced to $\gamma = \gamma_L/3 = 1/\sqrt{2}$. Foam response with different phase angles has been observed for Kelvin foams (Reinelt & Kraynik 1996) and honeycombs (Kraynik & Hansen 1986).

VII. TIME-AVERAGED SHEAR STRESS

The time-averaged stresses evaluated from (8) are presented in Table II. Equations (6) and (7) give consistent results for the shear stress component σ_{xy}. The average shear stress was 0.119, 0.204, and 0.617 for three different orientations of a Kelvin foam (Reinelt & Kraynik 1996). The highest value includes a triple transition, which causes large stress. The TCP results that do not involve Kelvin cells show less variation in average shear stress than those that do.

VIII. CONCLUSIONS

The microrheology of Weaire-Phelan and Friauf-Laves foams exhibits all of the features expected of dry foams in quasistatic shearing flow. This includes piecewise-continuous stress-strain functions whose branches correspond to nonlinear elastic behavior, branches terminating when the foam structure violates Plateau's laws, and irreversible cascades of local topology transitions that reduce energy and restore stability.

Unlike the Kelvin foam, which can be modeled as one polyhedron in a unit cell, TCP foams require multiple polyhedra and consequently are far less constrained. Individual polyhedra change type as T1 cascades produce foams that contain a much greater variety of polyhedra and faces than existed originally. This occurs because individual faces, which begin as pentagons or hexagons, can gain or lose one or two edges. The first cascade alone can result in polygons ranging from triangles to octagons and they can be assembled to form many different polyhedra.

Single-cell simulations constrain each polyhedron 'to go with the (mean) flow.' Multiple cells eliminate this constraint and enable individual cells to move 'off lattice' and this, for example, enables shuffling. Without shuffling, the foam-response period would be several times the lattice period. With shuffling, they can be equal.

Eventually, all of the foams reorder because their response is strain-periodic. In some

cases the foams return to their original topology. In other cases they become Kelvin cells; but subsequent T1 cascades can result in disorder. This was observed in all cycles that include Kelvin cells. A T1 cascade begins with a cell edge going to zero length as strain increases. The process by which edges vanish in Kelvin foams and in TCP foams can be smooth and continuous, or abrupt and discontinuous. When multiple cells are involved, abrupt onset is often connected with symmetry-breaking bifurcations. The resulting structures have lower stress and less energy than their more symmetric counterparts. These bifurcations provide a mechanism for Kelvin cells to disorder. They can also cause strain localization; *e.g.*, in WP2b, a T1 cascade results in layers, two Kelvin cells thick, sliding past one another.

The magnitude of stress-strain fluctuations is just as large in the TCP foams as in Kelvin foams. Despite their complexity, the TCP foams are still small systems. The most elementary T1 transitions involve five cells and a particular cell can be altered several times during a T1 cascade. Consequently, the disturbance to the foam structure and the corresponding jumps in stress and energy are large. While it is very common to get negative shear stress during flow of a Kelvin foam, the shear stress was always positive when the response did not include Kelvin cells. This trend is favorable since negative shear stress is not anticipated during steady flow of large random foams. Results from 2D simulations suggest that it will probably require random foams with hundreds of cells to significantly reduce stress fluctuations (Weaire & Fu, 1988; Herdtle, 1991; Weaire & Fortes, 1994). Gopal & Durian (1995) have used a multiple-light scattering technique called diffusing-wave spectroscopy (DWS) to study nonlinear bubble dynamics during foam flow. They observed localized stick-slip like rearrangement of bubbles that undoubtedly refers to T1 cascades. The simulation of large random foams will provide connections with DWS experiments.

Acknowledgements

We thank Ken Brakke for developing and maintaining the Surface Evolver. Sandia is a multiprogram laboratory operated by Sandia Corporation, a Lockheed Martin Company, for the the U.S. Department of Energy under contract #DE-AC04-94AL85000.

REFERENCES

Brakke, K. A., "The surface evolver," Experimental Mathematics **1**, 141–165 (1992).

Gopal, A. D., and D. J. Durian, "Nonlinear bubble dynamics in a slowly driven foam," Phys. Rev. Lett. **75**, 2610–2613 (1995).

Herdtle, T., *Numerical studies of foam dynamics*. PhD Thesis, University of California at San Diego, La Jolla, CA (1991).

Kelvin, Lord (W. Thompson), "On the division of space with minimum partitional area," Philos. Mag. **24**, 503–514 (1887).

Kraynik, A. M. and M. G. Hansen, "Foam and emulsion rheology: A quasistatic model for large deformations of spatially-periodic cells," J. Rheology **30**, 409–439 (1986).

Kraynik, A. M. and D. A. Reinelt, "Elastic-plastic behavior of a Kelvin foam," Forma **11**, 255–270 (1996). Also published in "The Kelvin problem: Foam structures of minimal surface area," (ed. D. Weaire), Taylor & Francis Ltd., London, 93-108 (1996).

Plateau, J. A. F., *Statique Experimentale et Theorique des Liquides Soumis aux Seules Forces Moleculaires*, Gauthier-Villiard (1873).

Princen, H. M., "Rheology of foams and highly concentrated emulsions: I. Elastic properties and yield stress of a cylindrical model system," J. Coll. Int. Sci. **91**, 160–175 (1983).

Reinelt, D. A. and A. M. Kraynik, "Large elastic deformations of three-dimensional foams and highly concentrated emulsions," J. Coll. Int. Sci. **311**, 327–343 (1996).

Reinelt, D. A. and A. M. Kraynik, "Simple shearing flow of a dry Kelvin soap foam," J. Fluid Mech. **311**, 327–343 (1996).

Rivier, N., "Kelvin's conjecture on minimal froths and the counter-example of Weaire and Phelan," Phil. Mag. Lett. **69**, 297–303 (1994).

Schwarz, H. W., "Rearrangements in polyhedric foam," Recueil **84**, 771–781 (1964).

Taylor, J. E., "The structure of singularities in soap-bubble-like and soap-film-like minimal surfaces," Ann. Math. **103**, 489–539 (1976).

Weaire, D., and M. A. Fortes, "Stress and strain in liquid and solid foams," Advances in Physics, **43**, 685–738 (1994).

Weaire, D., and T-L. Fu, "The mechanical behavior of foams and emulsions," J. Rheology **32**, 271–283 (1988).

Weaire, D. and R. Phelan, "A counter-example to Kelvin's conjecture on minimal surfaces," Phil. Mag. Lett. **69**, 107–110 (1994).

FIGURES

FIG. 1. Kelvin cell and two TCP structures, Weaire-Phelan (A15) and Friauf-Laves (C15), showing the polyhedra in a representative volume (unit cell) of foam.

FIG. 2. The fundamental topological transition is reversible. A vanishing edge produces a triangular face (ET), and its reverse, a vanishing triangular face produces a new edge (TE). The lines labeled 'f' designate cell edges in the foreground and 'b' refers to the background.

FIG. 3. The QQ transition 'rotates' a quadrilateral face; the one on the left lies in the plane of the page and the one on the right is nearly perpendicular. An ET transition followed by a TE transition would produce the same result.

FIG. 4. Energy cross sections leading to bifurcation of foam structure. A local minimum becomes a saddle point as strain increases.

FIG. 5. Deformed Weaire-Phelan foams viewed from two directions. From top to bottom $\gamma = 0, 0.30$, and 0.65 (just before the first topological transition).

FIG. 6. Shear stress σ_{xy} as a function of shear strain γ for orientation 1 of the Weaire-Phelan foam (WP1). The stress scale is $T/V^{1/3}$ in all figures. The solid bar represents the period of the foam response γ_F.

FIG. 7. First normal stress difference $N_1 = \sigma_{xx} - \sigma_{yy}$ (solid curves) and second normal stress difference $N_2 = \sigma_{yy} - \sigma_{zz}$ (dashed curves) as a function of strain for WP1.

FIG. 8. Shear stress as a function of strain for WP2a.

FIG. 9. Shear stress as a function of strain for WP2b. The solid bar represents the foam period γ_F and the dashed bar represents the lattice period γ_L. The label 'k' indicates those branches that only involve Kelvin cells.

FIG. 10. Shear stress as a function of strain for Friauf-Laves orientations FL1a and FL1b. The only difference between the two is indicated by the dotted lines.

FIG. 11. Shear stress as a function of strain for FL1c.

FIG. 12. Shear stress as a function of strain for Friauf-Laves orientation 2; FL2a starts at $\gamma = 0$ and FL2b starts at $\gamma = 1/\sqrt{2}$ as indicated by the dashed line.

TABLES

TABLE I. Structure evolution for WP1. Columns labeled 3-10 contain the number of faces with p edges. Columns labeled D_1-Z_2 show how a particular polyhedron gains and loses faces as the foam deforms and undergoes topological transitions. Rows beginning with a range of strain refer to stable structures that persist until the next T1 cascade. The † refers to the positions occupied by a particular polyhedron at the end of the cycle; *e.g.*, dodecahedron D_2 becomes Y_1, a 14-hedron in the y-column, and the original Y_1 moves to D_2, *i.e.*, D_2 and Y_1 shuffle within the lattice. The ‡ indicates final positions for an alternate bifurcation path.

	faces with p edges								faces on a particular cell							
γ	3	4	5	6	7	8	9	10	D_1	D_2	X_1	X_2	Y_1	Y_2	Z_1	Z_2
0-0.70	0	0	48	6	0	0	0	0	12	12	14	14	14	14	14	14
	2	5	34	14	0	1	0	0	14	12	15	15	14	14	14	14
0.70-0.98	0	14	22	18	2	0	0	0	18	16	13	13	14	14	12	12
	6	14	16	15	6	2	0	1	18	16	15	15	14	14	14	14
0.98-1.10	0	17	20	16	4	1	0	0	16	16	14	14	14	14	14	14
	3	15	19	14	6	2	0	0	16	17	14	14	14	15	14	14
	0	15	23	15	3	1	0	0	16	17	14	14	12	15	13	13
	1	13	24	15	3	1	0	0	16	17	14	12	14	13	14	14
	0	11	30	11	4	0	0	0	16	16	14	12	14	12	14	14
	0	8	35	10	3	0	0	0	14	14	14	14	14	14	14	14
	3	6	32	13	1	2	0	0	14	14	14	14	15	15	14	14
	0	6	37	11	1	0	0	0	14	12	14	14	15	15	13	13
	1	2	42	9	1	0	0	0	12	14	14	14	13	15	14	14
1.10-1.70	0	0	48	6	0	0	0	0	12	14	14	14	12	14	14	14
									† D_1	Y_1	X_2	X_1	D_2	Y_2	Z_1	Z_2
									‡ D_1	Y_2	X_2	X_1	Y_1	D_2	Z_1	Z_2

TABLE II. Average shear stress $\overline{\sigma}_{xy}$ and the normal stress differences, $\overline{N}_1 = \overline{\sigma}_{xx} - \overline{\sigma}_{yy}$ and $\overline{N}_2 = \overline{\sigma}_{yy} - \overline{\sigma}_{zz}$. Orientations that involve Kelvin cells are denoted by (K). Stress is scaled by $T/V^{1/3}$.

Orientation	$\overline{\sigma}_{xy}$	$\overline{N}_1$	$\overline{N}_2$
WP1	0.354	0.212	-0.172
WP2a	0.296	0.092	-0.042
WP2b (K)	0.272	-0.112	0.106
FL1a,b (K)	0.498	0.106	-0.098
FL1c (K)	0.054	0.299	-0.194
FL2a,b	0.436	0.289	-0.210

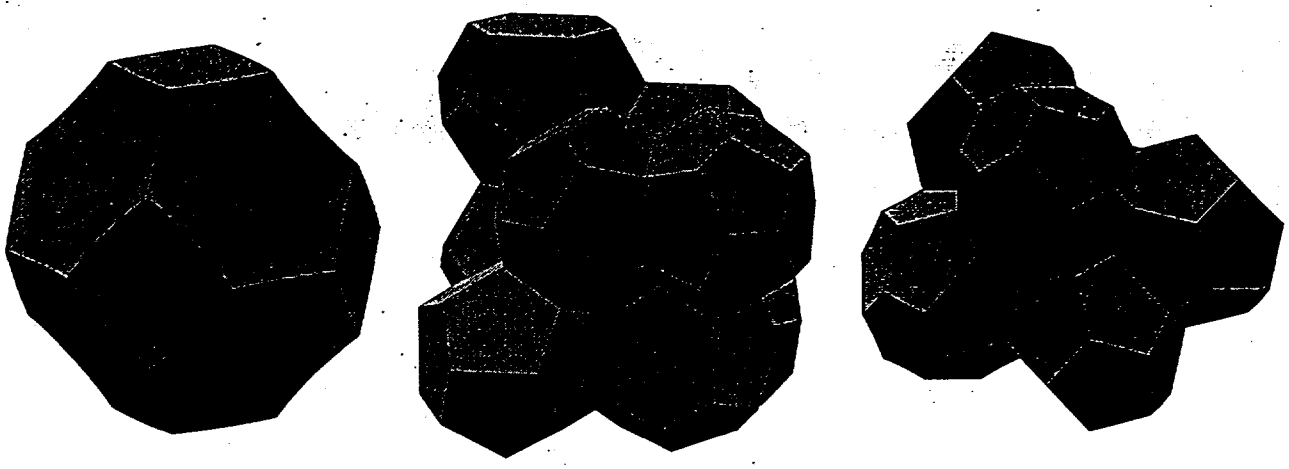

FIG 1

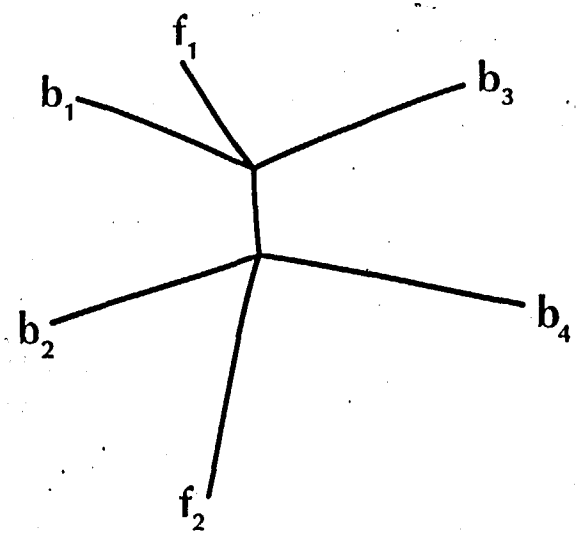

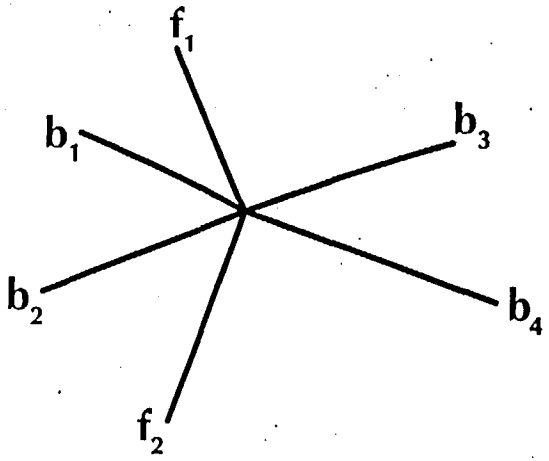

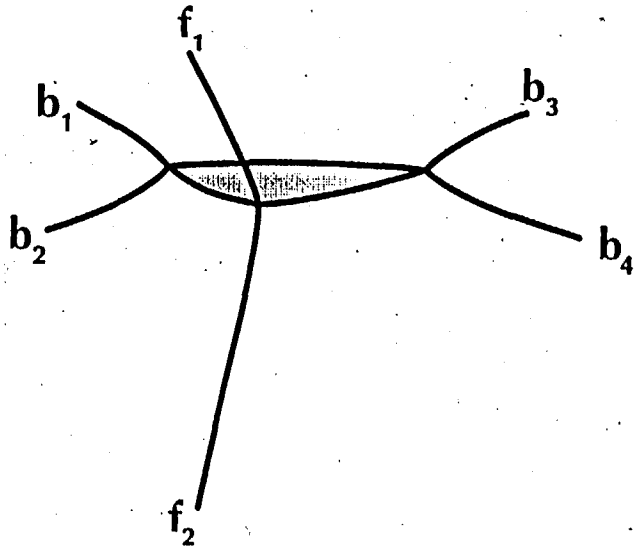

FIG 2

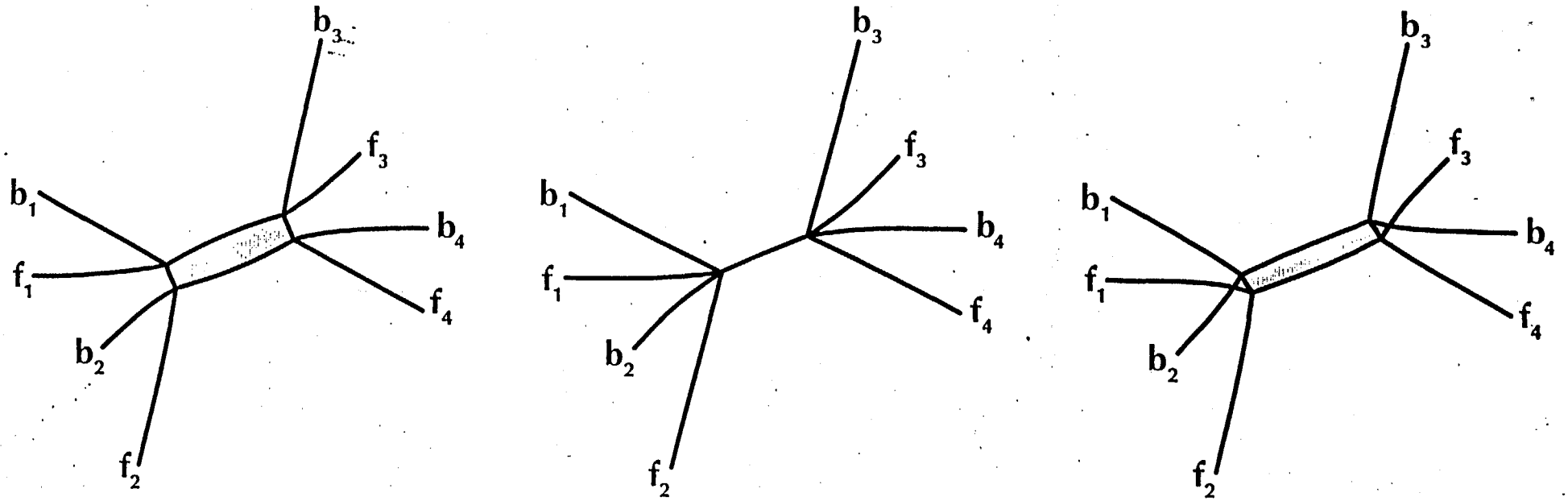

FIG 3

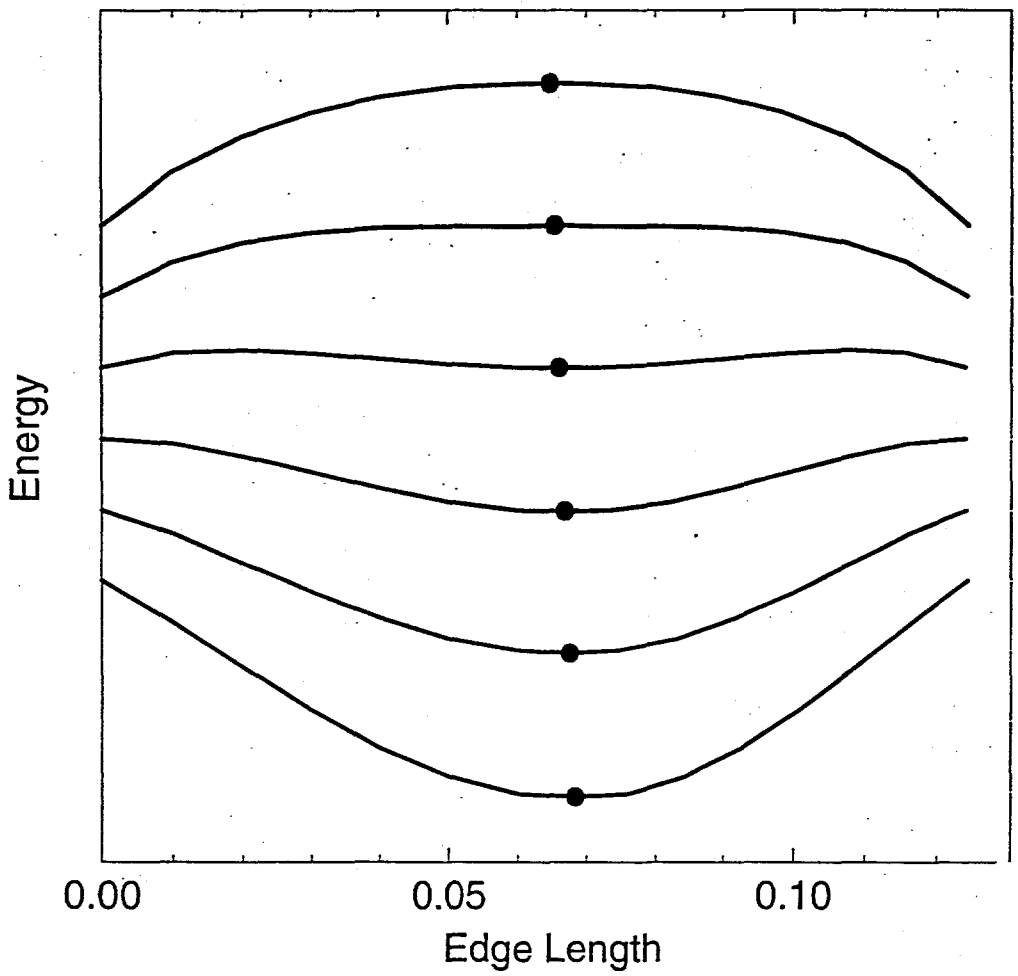

FIG 4

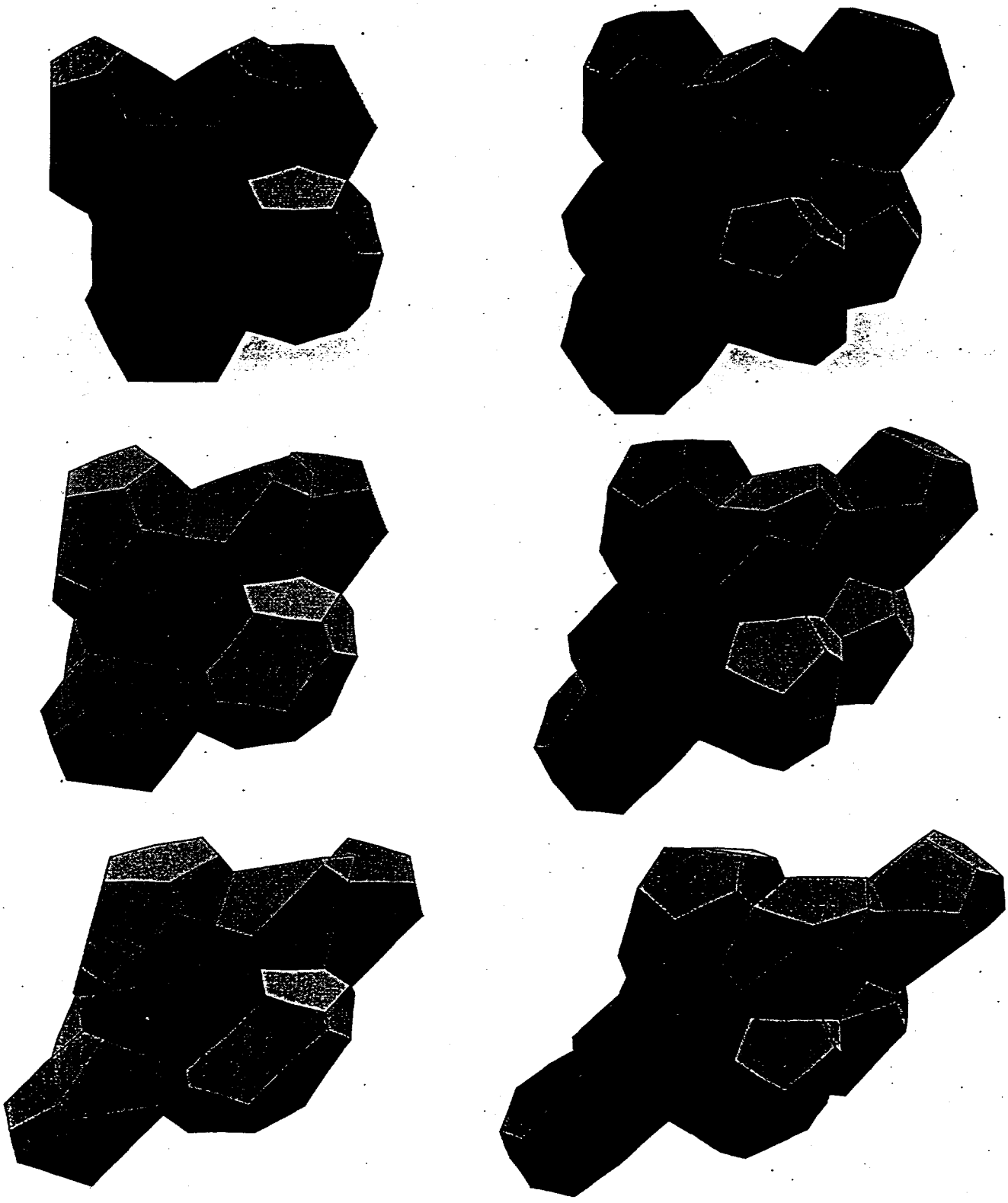

FIG 5

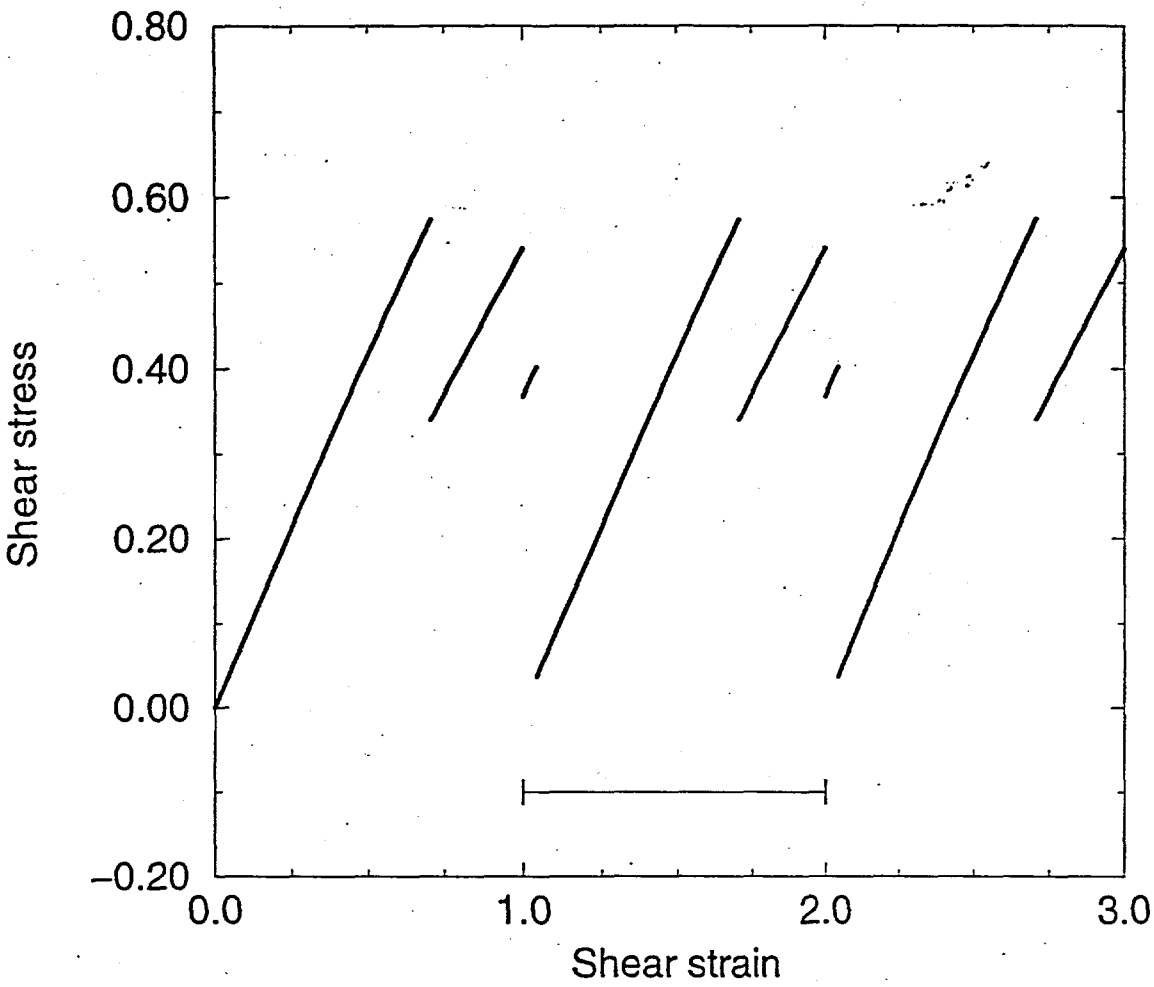

FIG 6

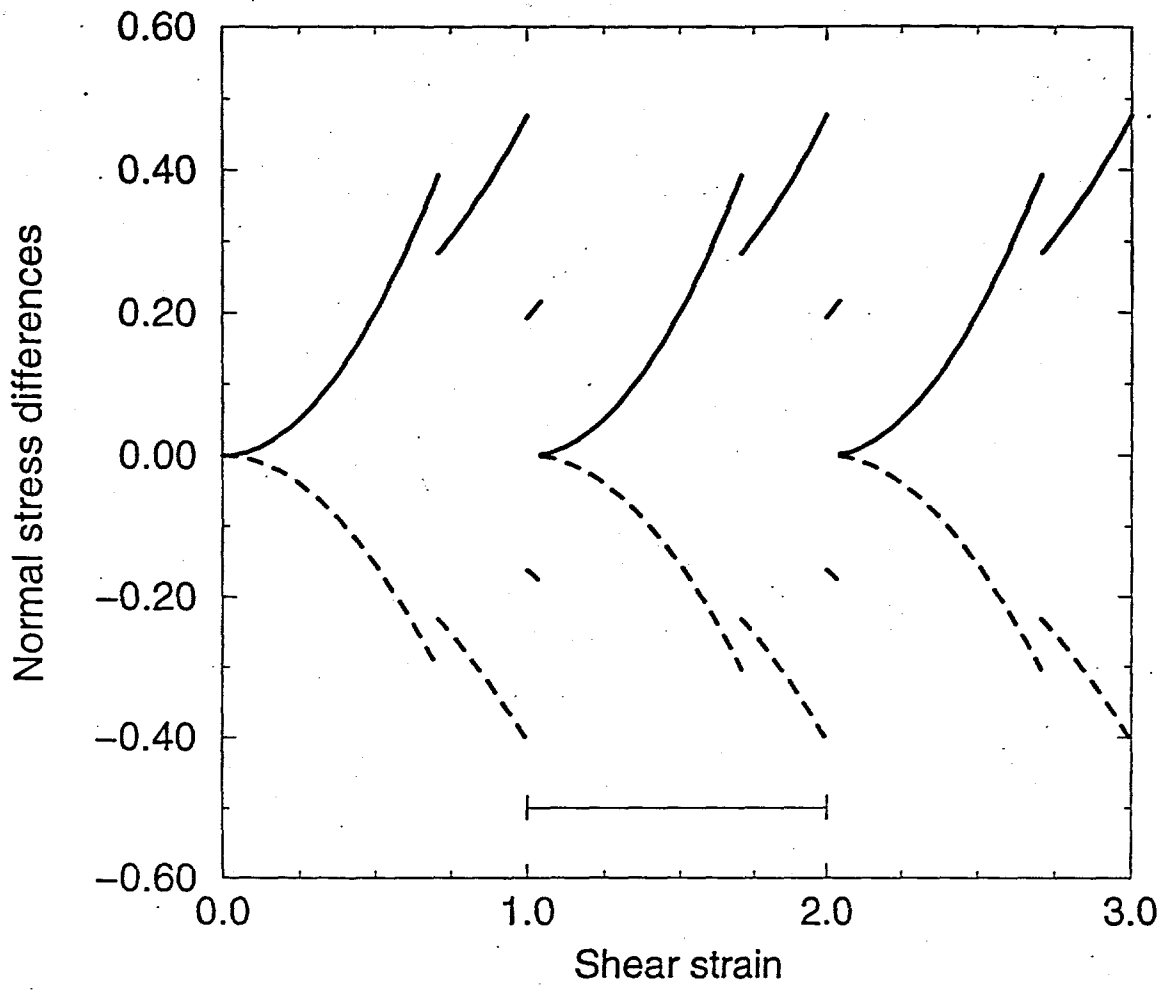
0.60
0.40
0.20
0.00
−0.20
−0.40
−0.60
Normal stress differences
0.0
1.0
2.0
3.0
Shear strain

FIG 7

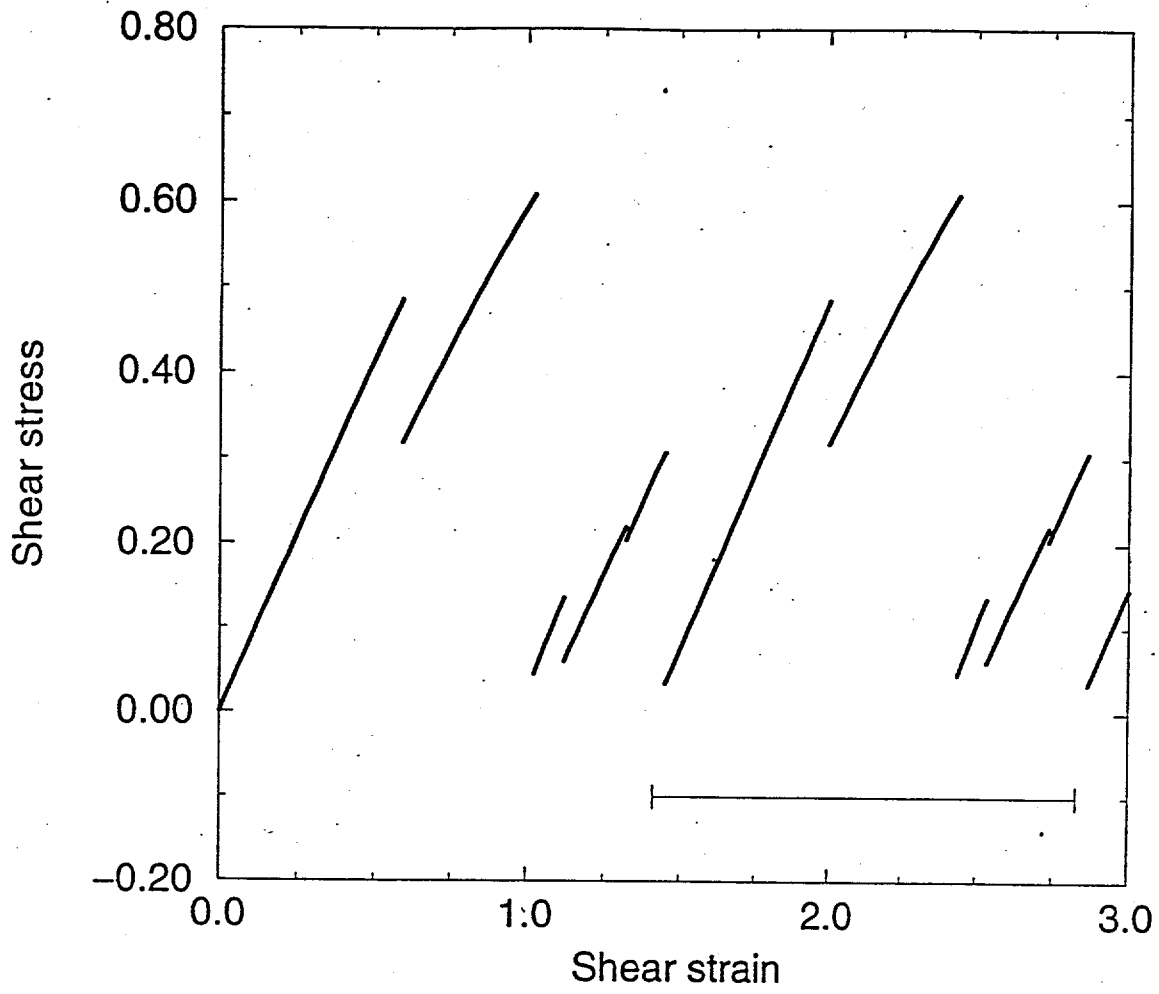

FIG 8

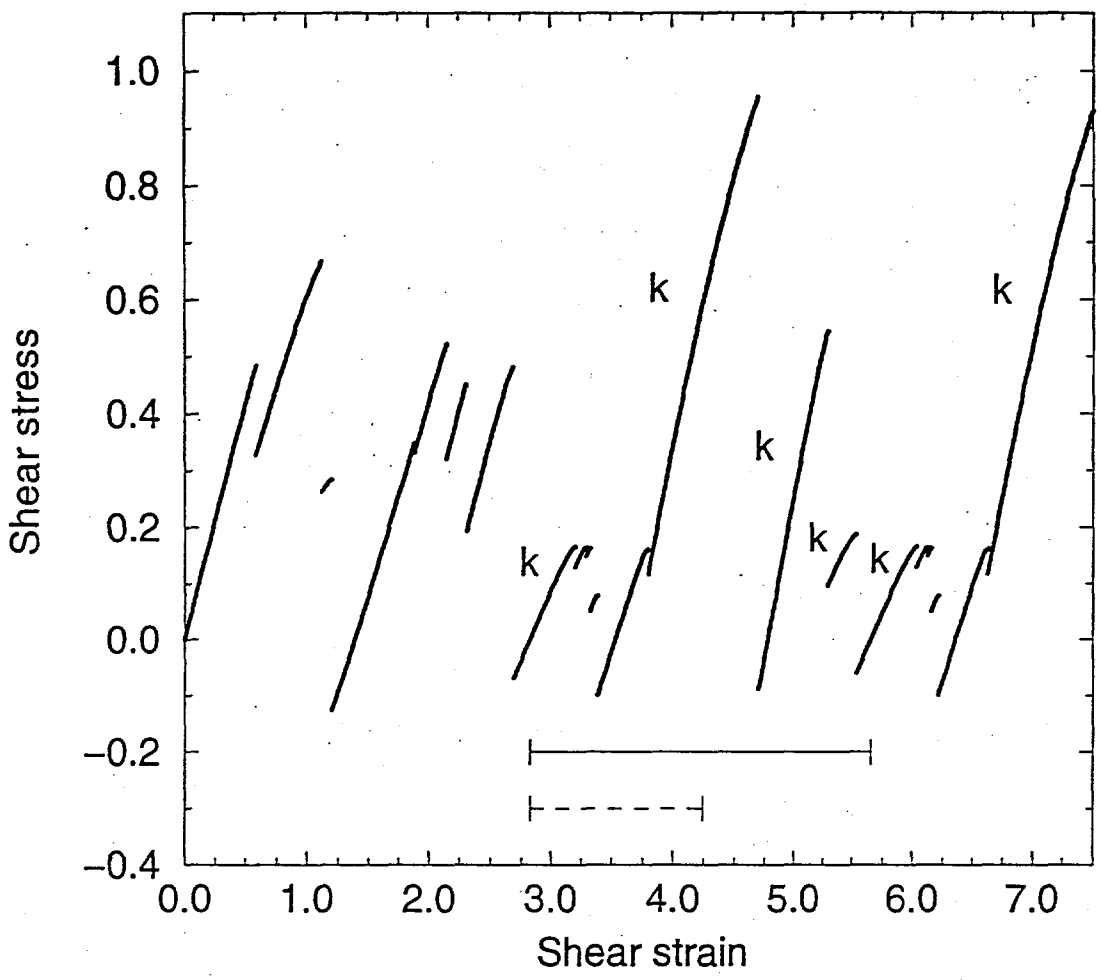
1.0
0.8
0.6
0.4
0.2
0.0
−0.2
−0.4
Shear stress
0.0
1.0
2.0
3.0
4.0
5.0
6.0
7.0
Shear strain
k
k
k
k
k
k

FIG 9

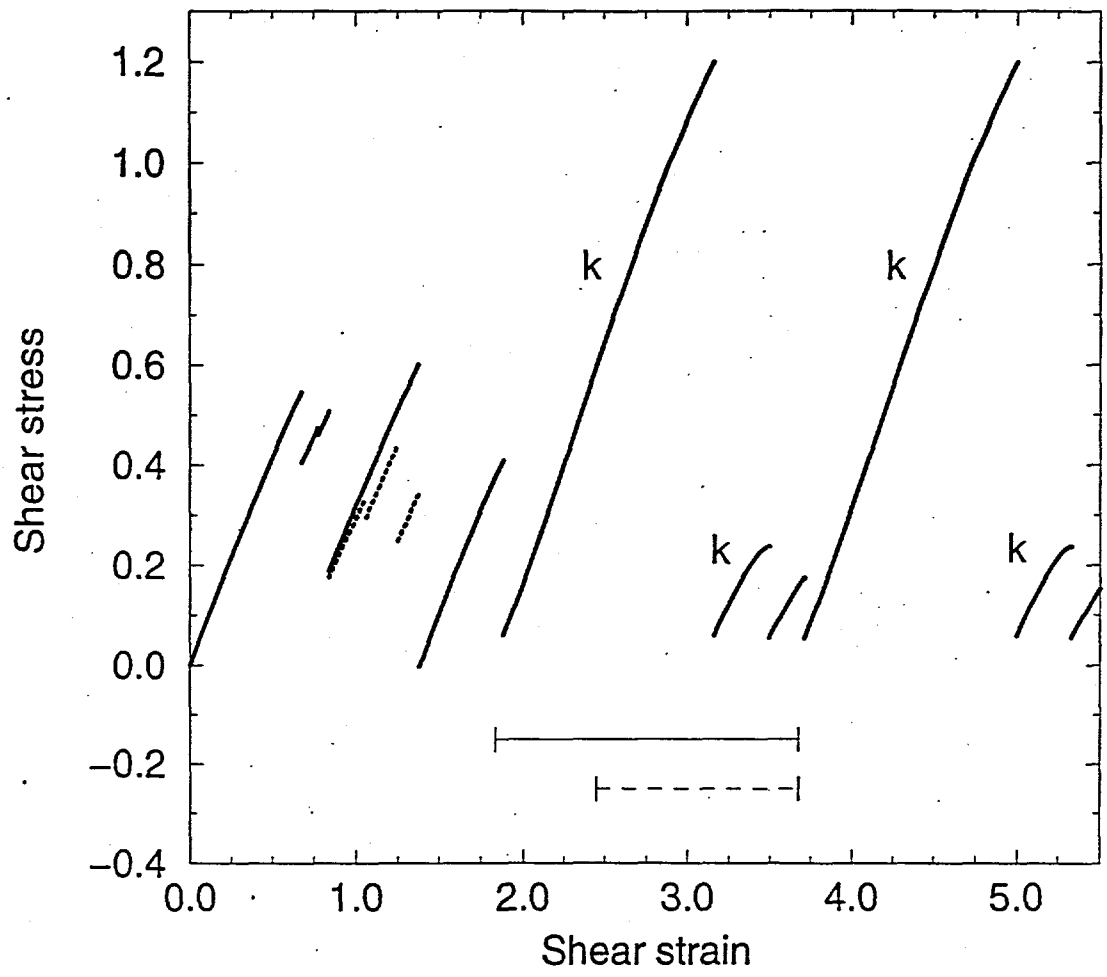
1.2
1.0
0.8
0.6
0.4
0.2
0.0
−0.2
−0.4
Shear stress
k
k
k
k
0.0
1.0
2.0
3.0
4.0
5.0
Shear strain

FIG 10

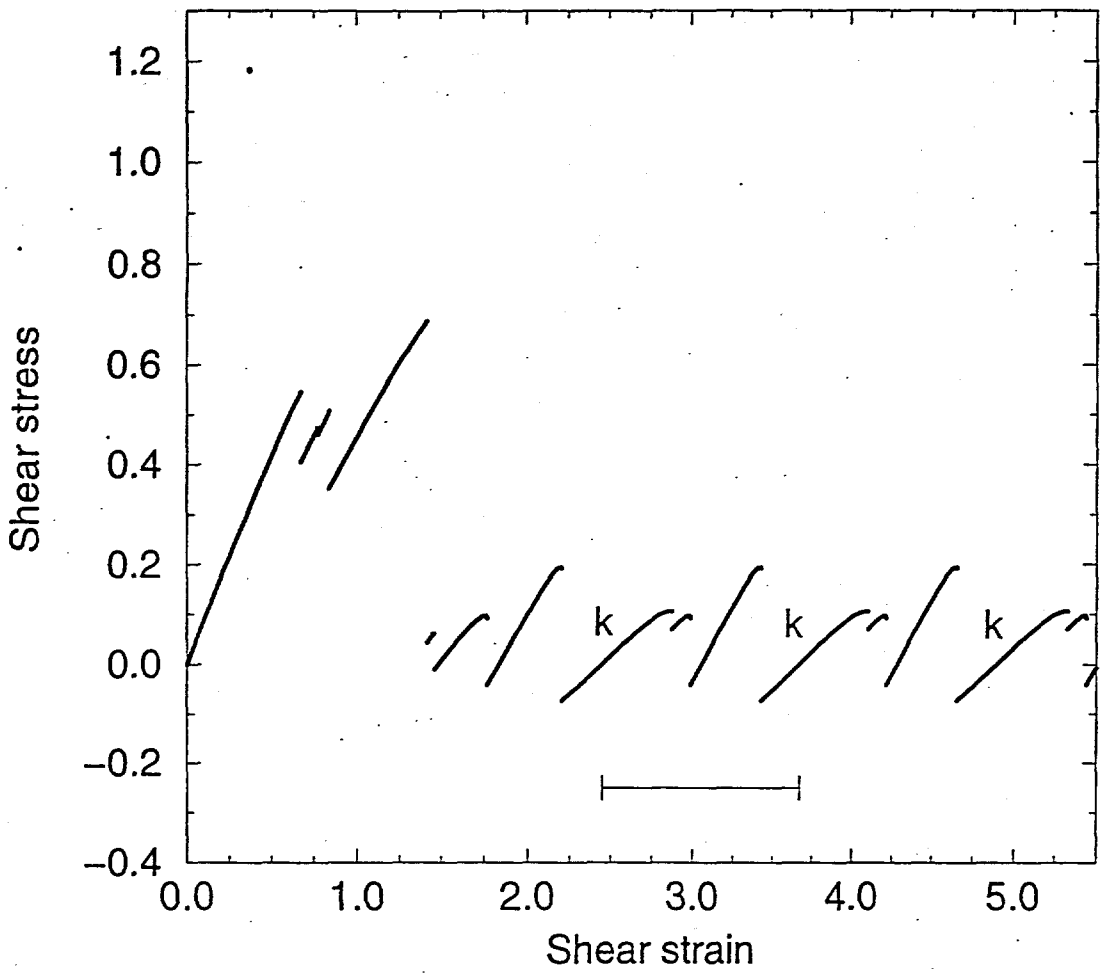
1.2
1.0
0.8
0.6
0.4
0.2
0.0
−0.2
−0.4
Shear stress
0.0
1.0
2.0
3.0
4.0
5.0
Shear strain
k
k
k

FIG 11

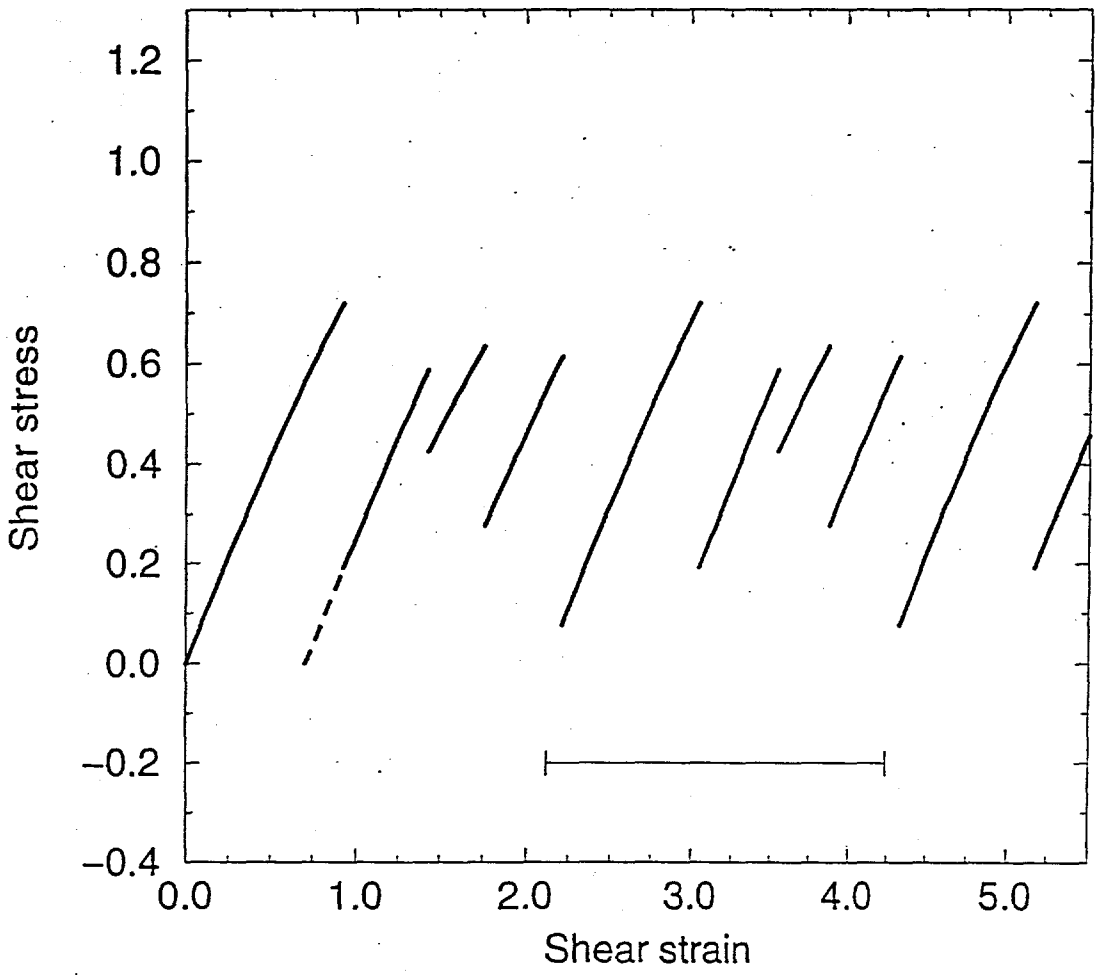
1.2
1.0
0.8
0.6
0.4
0.2
0.0
−0.2
−0.4
Shear stress
0.0
1.0
2.0
3.0
4.0
5.0
Shear strain

FIG 12